

Redshift evolution of stellar mass versus gas fraction relation in $0 < z < 2$ regime: observational constraint for galaxy formation models

Kana Morokuma-Matsui^{1,2*} and Junichi Baba³

¹*Nobeyama Radio Observatory, National Astronomical Observatory of Japan, 462-2 Nobeyama, Minamimaki, Minamisaku, Nagano 384-1305, Japan*

²*Chile Observatory, National Astronomical Observatory of Japan, 2-21-1 Osawa, Mitaka, Tokyo 181-8588, Japan*

³*Earth-Life Science Institute, Tokyo Institute of Technology, 2-12-1 Ookayama, Meguro-ku, Tokyo, 152-8550, Japan*

Accepted 1988 December 15. Received 1988 December 14; in original form 1988 October 11

ABSTRACT

We investigate the redshift evolution of the molecular gas mass fraction ($f_{\text{mol}} = \frac{M_{\text{mol}}}{M_{\star} + M_{\text{mol}}}$, where M_{mol} is molecular gas mass and M_{\star} is stellar mass) of galaxies in the redshift range of $0 < z < 2$ as a function of the stellar mass by combining CO literature data. We observe a stellar-mass dependence of the f_{mol} evolution where massive galaxies have largely depleted their molecular gas at $z = 1$, whereas the f_{mol} value of less massive galaxies drastically decreases from $z = 1$. We compare the observed $M_{\star} - f_{\text{mol}}$ relation with theoretical predictions from cosmological hydrodynamic simulations and semi-analytical models for galaxy formation. Although the theoretical studies approximately reproduce the observed mass dependence of f_{mol} evolution, they tend to underestimate the f_{mol} values, particularly of less massive ($< 10^{10} M_{\odot}$) and massive galaxies ($> 10^{11} M_{\odot}$) when compared with the observational values. Our result suggests the importance of the feedback models which suppress the star formation while simultaneously preserving the molecular gas in order to reproduce the observed $M_{\star} - f_{\text{mol}}$ relation.

Key words: galaxies: evolution – galaxies: ISM – radio lines: ISM

1 INTRODUCTION

Current galaxy-formation models are constructed so as to reproduce the observed *stellar* mass function (SMF) of galaxies. The statistical properties of the stellar components of galaxies have been investigated by means of large surveys in the optical and near-infrared wavelengths (e.g. Cole et al. 2001; Kochanek et al. 2001). It is known that the galaxy formation models based on the canonical cold dark matter hypothesis (the so-called Λ CDM hypothesis) overpredict the number densities of less massive and massive galaxies when compared with the observed SMFs of galaxies (e.g. Benson et al. 2003). To resolve this discrepancy, several feedback processes have been proposed to blow-out and/or heat up the cold-gas component, which is the raw material for star formation (e.g. Silk & Mamon 2012; Somerville & Davé 2014). For low-mass galaxies, the feedback processes of the blowing-out of the cold gas by supernovae (SNe; e.g. Larson 1974; Dekel & Silk 1986), photoionisation by cosmic ultraviolet background radiation (e.g. Ikeuchi 1986; Efstathiou 1992; Navarro & Steinmetz 1997;

Gnedin 2000; Okamoto et al. 2008), and preheating of the intergalactic medium (IGM) by gravitational pancaking (e.g. Mo et al. 2005; Lu et al. 2015) have been considered, while for high-mass galaxies, active galactic nucleus (AGN) feedback (e.g. Croton et al. 2006) and gravitational heating (e.g. Rees & Ostriker 1977; Khochfar & Ostriker 2008) have been considered.

Galaxy formation is a complex process which involves *both* stars and gas, and therefore, galaxy formation models are required to reproduce the observed properties of not only stellar but also the cold-gas components of galaxies. The observed mass-metallicity relation of galaxies implies that a galaxy is not a closed-box system, but evolves with the continual cycling of baryons between galaxies and the IGM (e.g. Tremonti et al. 2004). Such a picture of galaxy evolution is supported by recent cosmological hydrodynamic simulations (Davé et al. 2011a,b). In such a galaxy-IGM ecosystem context, galaxies are described as a slowly evolving system (i.e. ‘quasi-equilibrium’ model; Bouché et al. 2010; Davé et al. 2012), where the galaxies acquire gas from cosmic large-scale filamentary structures (e.g. Kereš et al. 2005; Dekel et al. 2009) which activate star formation, lose gas by strong and ubiquitous outflows which regulate star forma-

* E-mail: kana.matsui@nao.ac.jp; babajn@elsi.jp

tion, and again acquire the gas returned from the halo (i.e. wind recycling; Oppenheimer et al. 2010). Therefore, investigations of the evolution of the gas component in galaxies are essential to understand galaxy formation.

Observations of cold-gas components in higher-redshift galaxies are currently underway. The cold-gas components, atomic hydrogen gas (H I) and molecular hydrogen gas (H_2), are traced by the 21-cm hyperfine structure line and the 3-mm line from the carbon monoxide (CO) rotational transition, respectively. Although most H I emission studies¹ in high redshift have been limited to the $z \approx 0.1 - 0.2$ regime due to instrumental frequency coverage and sensitivity (Catinella et al. 2008; Freudling et al. 2011; Fernández et al. 2013; Rhee et al. 2013), emissions from CO have been detected farther out to $z \sim 6$; these emissions have been used to measure the H_2 mass in the high- z universe (Carilli & Walter 2013, and references therein). Recent CO surveys of both local and high- z galaxies have revealed molecular gas fractions as a function of stellar mass (Saintonge et al. 2011a; Tacconi et al. 2013). In addition to these direct measurements of cold gas, newer advances in the observational studies of cold-gas components are also expected from other indirect methods based on the star-formation-rate-molecular-gas relation (e.g. Popping et al. 2012), dust continuum (Magdis et al. 2012a; Santini et al. 2014; Scoville et al. 2014, 2015), and the spectral features in the optical band (Morokuma-Matsui et al. 2015). These recent developments, as well as observations made with the newest generation of radio and sub-mm instruments such as ALMA (Atacama Large Millimeter/submillimeter Array), SKA (Square Kilometer Array), ASKAP (Australian Square Kilometre Array Pathfinder), MeerKAT, and NOEMA (NOthern Extended Millimeter Array) are expected to provide us important constraints on galaxy formation theories.

Recent cosmological galaxy formation models contain sufficient physical ingredients (e.g. gas cooling, H_2 formation, star formation, and feedback) such that direct comparison with observations is now possible. Although the statistical properties of galaxies have been studied with semi-analytical models (SAMs; e.g. Kauffmann et al. 1999; Somerville & Primack 1999; Cole et al. 2000; Nagashima et al. 2005), recent large-scale cosmological N -body/hydrodynamic simulations also allow us to statistically study galaxy formation and evolution (e.g. Schaye et al. 2010, 2015; Okamoto et al. 2014; Thompson et al. 2014; Vogelsberger et al. 2014). In addition, some of these theoretical studies have implemented the equilibrium or non-equilibrium formation of H_2 , as well as star formation from such H_2 gas, in cosmological simulations (Gnedin et al. 2009; Christensen et al. 2012; Thompson et al. 2014; Tomassetti et al. 2015) and SAMs (Lagos et al. 2011b; Fu et al. 2012; Popping et al. 2014; Somerville et al. 2015).

However, these theoretical models still require many ‘sub-grid’ parameters for star formation and feedback mod-

els due to limited spatial/mass resolutions and a lack of the full understanding of related physical processes (for more details, see a recent review by Somerville & Davé 2014). As described above, there are fewer studies on the evolution of the cold-gas component of galaxies than those on stellar components. Recent developments in both observational and theoretical studies on the galactic cold-gas components provide us a unique opportunity to compare theoretical and observational results and to obtain the constraints for theoretical models.

In this study, we investigate as to whether the current galaxy formation models reproduce the observed properties of the cold-gas components of galaxies by comparing the observed and theoretically predicted evolutions of the molecular gas mass fraction with respect to the total baryonic mass as a function of stellar mass. The outline of the paper is as follows. We first investigate the redshift evolution inferred from the observational data in section 2. In section 3, the observed redshift evolution is compared with the model predictions. Further, we discuss feedback models implemented in galaxy formation models in section 4. Finally, we summarise the study and comment on possible future prospects in this direction in section 5.

2 OBSERVED EVOLUTION OF MOLECULAR GAS FRACTION

In this section, we investigate the observed molecular gas fraction as a function of stellar mass. The molecular gas mass fraction is defined as

$$f_{\text{mol}} = \frac{M_{\text{mol}}}{M_{\text{mol}} + M_{\star}}, \quad (1)$$

where M_{\star} and M_{mol} denote the stellar mass and molecular gas mass of a galaxy, respectively. We combine the literature data of M_{\star} and M_{mol} and calculate the molecular gas mass fraction f_{mol} of various galaxies. The literature data of M_{mol} include both direct and indirect estimations. In the following sections, we first describe the literature data used in our study (sections 2.1 and 2.2) and we subsequently investigate the redshift evolution of f_{mol} as a function of stellar mass (section 2.3).

2.1 Measurement of molecular gas mass from CO

CO data were retrieved from nine studies (Leroy et al. 2008; Daddi et al. 2010; Geach et al. 2011; Saintonge et al. 2011a; Bauermeister et al. 2013; Tacconi et al. 2013; Boselli et al. 2014; Bothwell et al. 2014; Morokuma-Matsui et al. 2015) to cover a wide range of redshifts and stellar masses. We adopted the Galactic conversion factor of $\alpha_{\text{CO}} = 4.35 \text{ M}_{\odot} (\text{K km s}^{-1} \text{ pc}^2)^{-1}$ (including the contribution of helium; Bolatto et al. 2013) for all the sample galaxies² considered in this study to estimate the molecular gas mass as

$$M_{\text{mol}} = \alpha_{\text{CO}} L'_{\text{CO}}, \quad (2)$$

¹ The absorption line observations of neutral hydrogen are also used to test galaxy formation theories (Rahmati et al. 2013a,b; Rahmati & Schaye 2014; Rahmati et al. 2015; Bird et al. 2014; Berry et al. 2014).

² The starburst galaxies, which require different α_{CO} , are excluded in this study even though they were included in the original studies.

Name	Redshift z	M_\star ($10^{10} M_\odot$)	SFR (M_\odot/yr)	Symbols in figure 1	Reference
Ler08	0.0007 – 0.004	0.001 – 8.0	0.7 – 4.1	open square	Leroy et al. (2008)
Bos14	0.0035 – 0.006	0.03 – 13.1	0.01 – 6.0	cross	Boselli et al. (2014)
Bot14	0.01 – 0.03	0.03 – 1.0	0.16 – 4.0	open pentagon	Bothwell et al. (2014)
Sai11	0.025 – 0.05	1.0 – 32	0.07 – 40	dot	Saintonge et al. (2011a)
Bau13	0.05 – 0.3	4.0 – 30	3.4 – 88	filled square	Bauermeister et al. (2013)
Mor15	0.1 – 0.2	4.0 – 20	8.5 – 48	filled circle	Morokuma-Matsui et al. (2015)
Gea11	0.4	4.1 – 11	28 – 62	open circle	Geach et al. (2011)
Dad10	1.5	3.3 – 11	62 – 400	open triangle	Daddi et al. (2010)
Tac13	1.0 – 1.5, 2.0 – 2.3	0.6 – 17	26 – 480	filled triangle	Tacconi et al. (2013)
Pop12	0.5 – 2.0	0.01 – 100	–	dash-dot lines	Popping et al. (2012)

Table 1. Summary of samples from the literature. Estimations of M_\star and SFR in each study are described in section 2.1.

where L'_{CO} represents the luminosity of the $^{12}\text{CO}(J=1-0)$ line in units of $\text{K km s}^{-1} \text{ pc}^2$. The CO data of Leroy et al. (2008), Bothwell et al. (2014), Tacconi et al. (2013), and Daddi et al. (2010) are not based on $^{12}\text{CO}(J=1-0)$ observations but based on $^{12}\text{CO}(J=3-2)$ or $^{12}\text{CO}(J=2-1)$. The conversions to $^{12}\text{CO}(J=1-0)$ intensity assumed in these studies are described in the following lists. We discuss effects of variable α_{CO} on f_{mol} in section 3.2. The literature data of the CO observations are summarised in Table 1. We also describe the stellar mass and star formation rate (SFR) estimations of these literature data in the following list.

- Leroy et al. (2008): Leroy et al. combined the literature data of the CO maps of local galaxies ($3 < D < 30$ Mpc) including spiral and dwarf galaxies, $^{12}\text{CO}(J=2-1)$ data from HERACLES (Leroy et al. 2008) and $^{12}\text{CO}(J=1-0)$ data from BIMA SONG (Helfer et al. 2003). They assumed a $^{12}\text{CO}(J=2-1)$ to $^{12}\text{CO}(J=1-0)$ intensity ratio of 0.8. The stellar mass and SFR of the sample galaxies range over $10^{7.1} - 10^{10.9} M_\odot$ and $0.7 - 4.1 M_\odot \text{ yr}^{-1}$, respectively and they are the so-called main sequence of star-forming galaxies³. Leroy et al. derived stellar mass using Spitzer’s 3.6- μm data and SFR using GALEX FUV and Spitzer’s 24- μm data.

- Boselli et al. (2014): Boselli et al. observed $^{12}\text{CO}(J=1-0)$ emission data of 59 late-type galaxies of the Herschel Reference Survey, which is a survey of the complete K -band selected, volume-limited ($15 < D < 25$ Mpc) galaxies spanning a wide range in morphological type and luminosity, using the NRAO Kitt Peak 12-m telescope. They combined the literature data of CO and provided a CO catalogue of 225 out of the 322 galaxies of their complete sample with stellar mass of $10^{8.5} - 10^{11.2} M_\odot$ and SFR of $0.01 - 6 M_\odot \text{ yr}^{-1}$. The stellar masses of their samples were estimated in Cortese et al. (2012) from i -band luminosities using the $g-i$ colour-dependent stellar mass-to-luminosity ratio relation from Zibetti et al. (2009). The sample galaxies are the main sequence of star-forming galaxies (Cortese et al. 2014; Ciesla et al. 2014).

- Bothwell et al. (2014): Bothwell et al. presented the first data release of a $^{12}\text{CO}(J=2-1)$ survey with the 12-m telescope of Atacama Pathfinder Experiment (APEX) for

nearby dwarf galaxies at $0.01 < z < 0.03$ with the stellar mass and SFR ranges of $10^{8.5} - 10^{10} M_\odot$ and $0.1 - 4.0 M_\odot \text{ yr}^{-1}$, respectively. They limited to the samples with metallicity of $12 + \log(\text{O}/\text{H}) > 8.5$ for α_{CO} to be similar to or lower than the Milky Way value. They assumed a $^{12}\text{CO}(J=2-1)$ to $^{12}\text{CO}(J=1-0)$ intensity ratio of unity to estimate L'_{CO} . The stellar masses and SFRs of their sample galaxies were provided by the Max Planck Institute for Astrophysics-John Hopkins University (MPA-JHU) group. The stellar masses of the galaxies were derived by fitting the SDSS *ugriz* photometry to models spanning a wide range of star formation histories.

- Saintonge et al. (2011a): Saintonge et al. conducted a CO survey of local galaxies with stellar masses of $(1-30) \times 10^{10} M_\odot$ and SFRs of $0.07 - 40 M_\odot \text{ yr}^{-1}$ with the 30-m telescope at the IRAM facility (CO Legacy Data base for the GASS survey, COLD GASS), and their targets were selected such that the resulting stellar mass distribution was roughly flat. In their study, the stellar mass and SFR of galaxies were estimated by fitting the GALEX (NUV and FUV) and SDSS photometries with the Bruzual & Charlot (2003) population synthesis code (Saintonge et al. 2011b). Their sample consists of the star forming galaxies and passive galaxies.

- Bauermeister et al. (2013): Bauermeister et al. targeted 31 star-forming galaxies with stellar masses in the range of $(4-30) \times 10^{10} M_\odot$ and SFRs in the range of $3 - 90 M_\odot \text{ yr}^{-1}$ at $z \sim 0.05 - 0.5$ and detected CO emissions from 24 galaxies using the Combined Array for Research in Millimeter-wave Astronomy (CARMA) facility (Evolution of molecular Gas in Normal Galaxies, EGNog). The sample galaxies in the ranges of $z \sim 0.05 - 0.32$ from which CO emission was detected were drawn from SDSS DR7 (Abazajian et al. 2009). The stellar mass and SFR of their sample galaxies were provided by the MPA-JHU group. This estimate was found to be comparable with the one obtained from stellar absorption features (Kauffmann et al. 2003). Further, SFRs were derived by fitting the fluxes of no less than five emission lines (Brinchmann et al. 2004). In this study, we only use the data of the normal star-forming galaxies of their sample.

- Morokuma-Matsui et al. (2015): Morokuma-Matsui et al. conducted CO observations of 12 galaxies with stellar masses of $(4-20) \times 10^{11} M_\odot$ and SFRs of $8.5 - 48 M_\odot \text{ yr}^{-1}$ in the $z \sim 0.1 - 0.2$ regime using the 45-m telescope at the Nobeyama Radio Observatory, and they detected CO emission from 8 galaxies. Similar to the case of Bothwell et al.

³ It is known that star-forming galaxies form a distinct sequence of SFR with M_\star (e.g. Noeske et al. 2007). The galaxies on this sequence are called ‘main sequence’ galaxies.

(2014) and Bauermeister et al. (2013), the stellar masses and SFRs of their samples were also obtained from the MPA-JHU group and drawn from SDSS DR10 (Ahn et al. 2014). They showed that their samples correspond to star-forming galaxies at the redshift.

- Geach et al. (2011): Geach et al. observed seven galaxies selected based on the basis of the 24- μm emission galaxies with masses of $(4 - 11) \times 10^{11} M_{\odot}$ and SFRs of $28 - 62 M_{\odot} \text{ yr}^{-1}$ at $z \sim 0.4$ using the IRAM Plateau de Bure Interferometer (PdBI) and detected CO emission from five galaxies. The stellar masses of their samples were estimated by fitting *BVRICK* photometry (Moran et al. 2007) to model spectral energy distributions (SEDs) using the *KCORRECT* software package, v4.2 (Blanton & Roweis 2007). The SFRs of their samples were derived from the far-infrared luminosity (Kennicutt 1998a) estimated from the 7.7- μm -line luminosity (Geach et al. 2009).

- Daddi et al. (2010): Their sample galaxies comprised the star-forming galaxies with a stellar mass range of $(3 - 11) \times 10^{10} M_{\odot}$ and SFR range of $62 - 400 M_{\odot} \text{ yr}^{-1}$ in the $1.4 < z < 2.5$ regime classified by using the *BzK* colour criterion (Daddi et al. 2004) with Spitzer imaging detection at 24 μm . They observed CO($J = 2 - 1$) of five galaxies with IRAM PdBI and estimated L'_{CO} by assuming a CO($J = 2 - 1$)-to-CO($J = 1 - 0$) conversion factor of 0.86 (Dannerbauer et al. 2009). The stellar mass was estimated via an empirical method with *BzK* photometry, which was calibrated with the mass estimates from multicolor photometry and SED fitting (Daddi et al. 2004). The SFRs of their samples were the averages of three SFRs estimated from dust-corrected UV, 24- μm emission, and 1.4-GHz radio fluxes (Daddi et al. 2010).

- Tacconi et al. (2013): Tacconi et al. conducted the largest CO survey of $z \sim 1 - 2$ galaxies with stellar mass of $(0.6 - 17) \times 10^{10} M_{\odot}$ and SFR of $26 - 480 M_{\odot} \text{ yr}^{-1}$ with the IRAM PdBI and detected CO emissions from 52 galaxies (IRAM Plateau de Bure High- z Blue Sequence Survey, PHIBSS). The stellar mass was estimated from SED fitting. The SFR estimate was based on the sum of the observed UV- and IR-luminosities for the $z \sim 1.2$ samples (Wuyts et al. 2011), and the extinction-corrected H α luminosities for the $z \sim 2.2$ samples (Kennicutt 1998a; Förster Schreiber et al. 2009; Mancini et al. 2011; Wuyts et al. 2011). Their sample follows the main sequence of star-forming galaxies at the redshift. They observed the luminosities of the $^{12}\text{CO}(J = 3 - 2)$ lines of galaxies and converted these data sets into the luminosity of $^{12}\text{CO}(J = 1 - 0)$ lines using a $^{12}\text{CO}(J = 1 - 0)/^{12}\text{CO}(J = 3 - 2)$ ratio of 2.

All the studies except for Leroy et al. (2008) assumed the Chabrier initial mass function (IMF, Chabrier 2003) for estimating the stellar mass and SFR of galaxies. Leroy et al. (2008) used Kroupa IMF (Kroupa 2001). We did not correct for this IMF difference, since the difference in the stellar mass and SFR estimations based on Chabrier and Kroupa IMFs is small compared to the other uncertainties (Chomiuk & Povich 2011; Kennicutt & Evans 2012; Madau & Dickinson 2014).

2.2 Estimation of molecular gas mass from SFR

We also use the molecular gas mass estimated indirectly from optical studies, since the CO measurement is limited to galaxies with a relatively narrow range of stellar mass ($\sim 10^{10} - 10^{11} M_{\odot}$), particularly at high redshift.

Popping et al. (2012) estimated the f_{mol} values of the COSMOS (Cosmological Evolution Survey; Scoville et al. 2007) galaxies using the molecular gas mass values inferred from the Kennicutt-Schmidt (K-S) law and the pressure-based H $_2$ formation model (Blitz & Rosolowsky 2004, 2006). They presented the fitting formulae of the $M_{\star} - f_{\text{mol}}$ relations for star-forming galaxies and all galaxies brighter than $I_{\text{AB}} = 24$ mag. For the star-forming galaxies, the fitting formula is given by

$$f_{\text{mol,P12,SF}} = \frac{1}{\exp(\log M_{\star} - A)/B + 1}, \quad (3)$$

where

$$A = 6.15 \left(1 + \frac{z}{0.036}\right)^{0.144}, \quad B = 1.47(1 + z)^{-2.23}, \quad (4)$$

and that for the whole galaxies brighter than 24 mag in I_{AB} is

$$f_{\text{mol,P12}} = \frac{1}{\exp(\log M_{\star} - C)/D + 1}, \quad (5)$$

where

$$C = 6.33 \left(1 + \frac{z}{0.016}\right)^{0.115}, \quad D = 1.71(1 + z)^{-1.57}. \quad (6)$$

Here, we mention that Popping et al. (2012) showed that their $I_{\text{AB}} < 24$ mag sample is complete (100 %) for the range of $10^{9.2} M_{\odot} < M_{\star} < 10^{11.7} M_{\odot}$ at $0.5 < z < 0.75$ with respect to the SMF derived in the same field (Ilbert et al. 2010). However, it is almost evenly $< 50\%$ for all stellar mass ranges at $z > 1.25$. In addition, if we assume the fitting functions of Popping et al. (2012) as accurate, the f_{mol} values of galaxies with stellar masses $> 10^{11} M_{\odot}$ becomes larger at lower redshifts, but the statistics with regards to higher- z massive galaxies in the fitting is poor. Thus, it is required to closely consider these observational limitations when we compare observations with theoretical studies.

2.3 Stellar-mass-dependent evolution of molecular gas mass fraction of galaxies

In this section, we investigate the stellar mass dependence of f_{mol} evolution using the observational data. Figure 1 shows the redshift evolution of the fraction f_{mol} as a function of stellar mass. Although the stellar mass range of galaxies with CO measurements is narrow at high redshift ($z > 0.1$), we can observe the stellar-mass dependence where the massive galaxies have smaller f_{mol} values than their less massive counterparts at $z \sim 0 - 2$. In all redshift ranges, the observed $M_{\star} - f_{\text{mol,CO}}$ relations are well reproduced by the $M_{\star} - f_{\text{mol,P12,SF}}$ relations in which the molecular gas mass is estimated from the indirect method. Popping et al. (2012) have already reported that the $M_{\star} - f_{\text{mol,P12,SF}}$ relation succeeds in reproducing the observed $M_{\star} - f_{\text{mol,CO}}$ relations of local galaxies (Saintonge et al. 2011a) and $z \sim 1 - 2$ samples (Tacconi et al. 2010). Here, we found that their $M_{\star} - f_{\text{mol,P12,SF}}$ relation also reproduces the observed $M_{\star} - f_{\text{mol,CO}}$ relations of galaxies at $z \sim 0.1 - 1$.

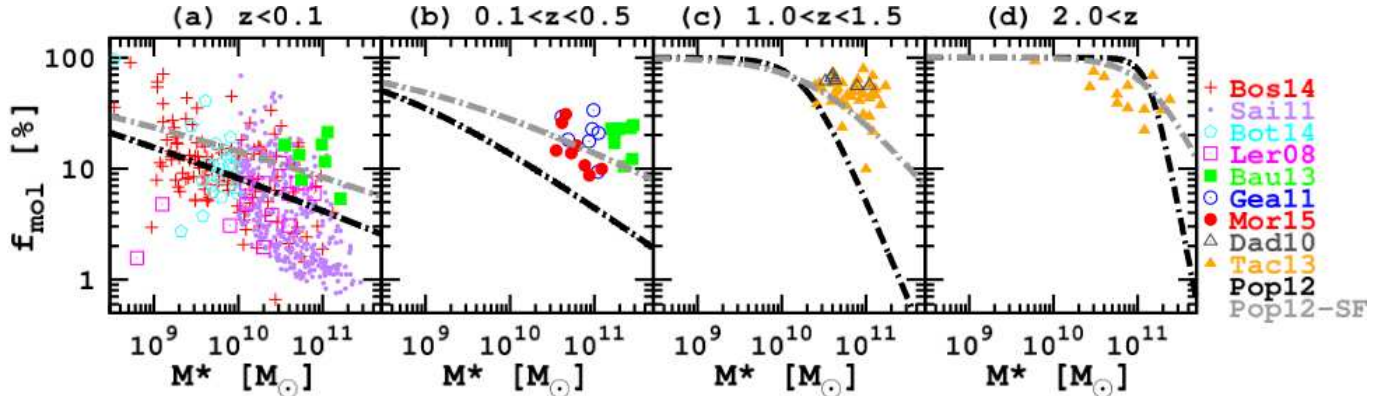


Figure 1. Molecular gas mass fraction f_{mol} as a function of stellar mass and redshift (a: $z < 0.1$, b: $0.1 < z < 0.5$, c: $1.0 < z < 1.5$ and d: $2.0 < z$). The symbols indicate CO data from the literature (cross: Boselli et al. (2014), open-square: Leroy et al. (2008), small-circle: Saintonge et al. (2011a), open pentagon: Bothwell et al. (2014), filled-square: Bauermeister et al. (2013), filled-circle: Morokuma-Matsui et al. (2015), open-circle: Geach et al. (2011), open-triangle: Daddi et al. (2010), and filled-triangle: Tacconi et al. (2013)). The grey and black dot-dash lines indicate $M_\star - f_{\text{mol}}$ relations based on the K-S law and pressure-based H_2 formation models for the star-forming galaxies ($f_{\text{mol,P12,SF}}$) and whole samples ($f_{\text{mol,P12}}$), respectively in Popping et al. (2012). The redshifts of the equations for $f_{\text{mol,P12,SF}}$ and $f_{\text{mol,P12}}$ are 0.025 for (a), 0.3 for (b), 1.25 for (c), and 2.2 for (d). The relationship between the symbols and references is summarised in Table 1. The stellar-mass-dependent f_{mol} evolution, where massive galaxies tend to reduce f_{mol} in earlier epochs compared to their less massive counterparts, can be clearly observed (see section 2.3 for more details).

There is a clear stellar-mass dependence in the f_{mol} evolution of star-forming galaxies where less massive galaxies tend to show a decrease in f_{mol} over time as reported in Popping et al. (2012, 2015). Here, we remark that recent dust-based studies have also suggested that the stellar-mass dependence of the cold gas mass fraction ($f_{\text{gas}} = \frac{M_{\text{gas}}}{M_{\text{gas}} + M_\star}$, where M_{gas} denotes the total cold gas mass including the atomic and molecular gas) shows a similar stellar-mass dependent evolution (Santini et al. 2014). Therefore, studies based on two independent methods (CO or dust) both suggest the stellar-mass dependent evolution of the cold gas fraction of galaxies.

We examine the stellar-mass dependent evolution of f_{mol} quantitatively. We must consider the stellar mass growth when discussing the f_{mol} evolution. If we adopt the stellar mass growth of star-forming galaxies as reported in Leitner (2012), the redshift evolution of the $M_\star - f_{\text{mol,P12,SF}}$ relation suggests that galaxies with stellar masses of $10^{10} M_\odot$, $10^{10.5} M_\odot$, and $10^{11} M_\odot$ at $z = 0$ exhibit decreases by factors of 8 (from 80 % to 10 %), 6 (37 % to 7.0 %), and 4 (26 % to 6.1 %) in their molecular gas mass fraction from $z = 1$ to $z = 0$, respectively⁴. Similarly, if we use the stellar mass growth of galaxies based on the abundance matching method (i.e. not biased with respect to star-forming galaxies; Conroy & Wechsler 2009), the $M_\star - f_{\text{mol,P12}}$ evolution suggests that the galaxies with stellar masses of 10^{10} , $10^{10.5}$, and $10^{11} M_\odot$ at $z = 0$ exhibit molecular gas-fraction decreases by factors of 14 (from 96 % to 6.8 %), 8 (14 % to 4.2 %), and 1 (4.9 % to 3.6 %) from $z = 1$ to $z = 0$, respectively. Therefore, the f_{mol} evolution of less massive galaxies in the range of $z = 0 - 2$ is more drastic than that of massive galaxies, and the massive galaxies appear to have depleted

relatively large fractions of their molecular gas by $z = 1$ ⁵ (Popping et al. 2015).

3 COMPARISON WITH THEORETICAL STUDIES

In this section, we compare the observed $M_\star - f_{\text{mol}}$ relation with predictions of theoretical studies constructed to reproduce the observed SMF. The theoretical studies we used in this study are briefly summarised in section 3.1. We demonstrate a discrepancy in the $M_\star - f_{\text{mol}}$ relation between the observations and theoretical predictions in section 3.2.

3.1 Galaxy formation models in the literatures

Recent galaxy formation models take into account star formation from molecular gas, as suggested by observations (e.g. Bigiel et al. 2008; Leroy et al. 2008). These theoretical models need to consider both star formation and molecule formation. Since star formation is an unknown process and the current cosmological numerical simulations of galaxy formation cannot resolve the spatial scale of molecular clouds, the galaxy formation models treat star formation as a ‘sub-grid’ model (see below).

For H_2 formation, most hydrodynamic simulations and SAMs adopt simplified methods such as ‘pressure-based’ and ‘metallicity-based’ models, although some cosmological hydrodynamic simulations solve the non-equilibrium chemical reactions of hydrogen (Gnedin et al. 2009). The

⁴ Here we use the $M_\star - f_{\text{mol,P12,SF}}$ relation because Leitner (2012) estimated the growth rate of stellar mass by assuming that present-day star-forming galaxies were on the ‘main sequence’ of the star-forming galaxies.

⁵ f_{mol} evolution farther out to $z = 3$ has been also investigated (Magdis et al. 2012b; Saintonge et al. 2013). Magdis et al. (2012b) detected a $\text{CO}(J = 3 - 2)$ emission from an infrared luminous Lyman break galaxy at $z = 3.2$ with a stellar mass of $2 \times 10^{11} M_\odot$. The estimated f_{mol} is 36 % suggesting that massive galaxies have flat evolution of f_{mol} at least in $1 < z < 3$.

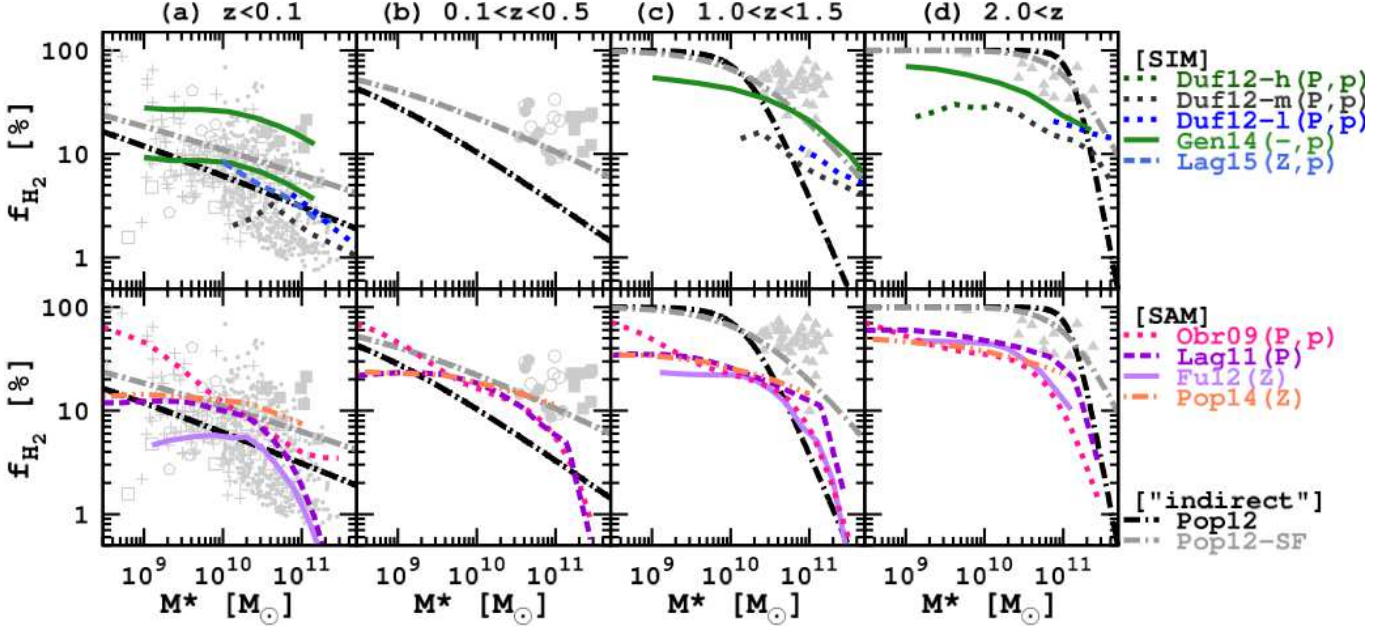


Figure 2. H_2 gas mass fraction f_{H_2} as a function of stellar mass and redshift (a: $z < 0.1$, b: $0.1 < z < 0.5$, c: $1.0 < z < 1.5$ and d: $2.0 < z$). The black and grey dot-dash lines indicate the $M_* - f_{H_2}$ relations based on the K-S law and pressure-based H_2 formation models for the star forming galaxies ($f_{H_2, P12, SF}$) and whole samples ($f_{H_2, P12}$), respectively in Popping et al. (2012). The redshifts of $f_{H_2, P12, SF}$ and $f_{H_2, P12}$ are 0.025 for (a), 0.3 for (b), 1.25 for (c), and 2.2 for (d). [Upper panel] Comparison with the predictions from cosmological N -body/hydrodynamic simulations (SIMs; dark-green, dark-grey, and blue dotted lines: high-, middle-, and low- resolution calculations of Duffy et al. (2012), respectively, solid green lines: Genel et al. (2014), and light-blue dashed lines: Lagos et al. (2015)). Genel et al. (2014) provided both lower and upper limits for f_{H_2} for galaxies at $z \sim 0$. [Lower panel] Comparison with the predictions from semi-analytic models (SAMs; pink dotted lines: Obreschkow et al. (2009), purple dashed lines: Lagos et al. (2011a), light-purple solid line: Fu et al. (2012), orange dot-dot-dashed line: Popping et al. (2014)). In the graph legend, ‘P’ denotes the pressure-based H_2 model, ‘Z’ denotes the metallicity-based H_2 model, and ‘p’ indicates that the H_2 model was implemented as a post-process. The relationship between the each symbol and the reference is summarized in Table 2. On each plot, we indicate the theoretical predictions for f_{H_2} at $z = 0$ in (a), $z = 0.5$ in (b), $z = 1$ in (c), and $z = 2$ in (d). Theoretical studies ‘qualitatively’ reproduce the stellar mass dependence of f_{H_2} evolution but there is a ‘non-negligible’ discrepancy between the observations and theoretical studies (see section 3.2 for details).

Label	Method	H_2 prescription	Star formation model	Feedbacks	Line Styles in Fig. 2	Reference
Duf12	SIM	Pressure*	Schaye & Dalla Vecchia (2008)	SN	dot	Duffy et al. (2012)
Gen14	SIM	—*	Springel & Hernquist (2003)	SN & AGN	solid	Genel et al. (2014)
Lag15	SIM	Metallicity [†] *	Schaye & Dalla Vecchia (2008)	SN & AGN	dash	Lagos et al. (2015)
Obr09	SAM	Pressure*	Kennicutt (1989)	SN & AGN	dot	Obreschkow et al. (2009)
Lag11	SAM	Pressure	Bigiel et al. (2008)	SN & AGN	dash	Lagos et al. (2011a,b)
Fu12	SAM	Metallicity	Bigiel et al. (2008)	SN & AGN	solid	Fu et al. (2012)
Pop14	SAM	Metallicity	Bigiel et al. (2008)	SN & AGN	dot-dot-dash	Popping et al. (2014)

Table 2. Summary of the theoretical studies used in Fig. 2. Details of each study are described in section 3.1. [†]The H_2 prescription is from Gnedin & Kravtsov (2011), which provided a fitting formula to their galaxy simulations incorporating non-equilibrium chemical network of hydrogen and helium and non-equilibrium cooling and heating rates. The other ‘Metallicity’ models use an analytical formula based on the chemical equilibrium model of H_2 (Krumholz et al. 2009a). * H_2 formation (partitioning) models were implemented as a post-process.

pressure-based model is an empirical method based on the observed relation between the molecule fraction of cold gas and the surface densities of stellar and gas components in nearby disc galaxies (Blitz & Rosolowsky 2004, 2006; Leroy et al. 2008). In contrast, the metallicity-based model uses an analytical formulae of the molecule fraction as a function of the gas density, metallicity, and radiation field (Krumholz et al. 2008, 2009a). It has been shown that both these types of models suitably reproduce the observed

molecular fraction of cold gas well (Blitz & Rosolowsky 2004, 2006; Krumholz et al. 2008; Fumagalli et al. 2010).

In this study, we compare the observations to the predicted $M_* - f_{mol}$ relations from three cosmological N -body/hydrodynamic simulations (SIM; Duffy et al. 2012; Genel et al. 2014; Lagos et al. 2015) and four SAMs (Obreschkow et al. 2009; Lagos et al. 2011a; Fu et al. 2012; Popping et al. 2014) of galaxy formation. We summarise the theoretical studies used in this study in Table 2.

- Duffy et al. (2012, SIM): Duffy et al. implemented the pressure-based H_2 formation model (Blitz & Rosolowsky 2006; Leroy et al. 2008) in the calculations of the Overwhelmingly Large Simulations (OWLS) project (Schaye et al. 2010) as a post-process. They determined the free parameters of the H_2 formation model according to recent observations (Leroy et al. 2008). Their estimated H_2 mass included the contribution of helium. The simulations in the OWLS include radiative cooling ($10^4 \text{ K} < T < 10^8 \text{ K}$ Wiersma et al. 2009), photoionisation heating from cosmic UV background radiation, star formation (Schaye & Dalla Vecchia 2008), mechanical feedback from SNe (i.e. by ‘kick’; Dalla Vecchia & Schaye 2008) and thermal feedback from AGN (Booth & Schaye 2009). Star formation is based on the study by Schaye & Dalla Vecchia (2008), in which they analytically recast the K-S law as a function of pressure rather than density, while assuming a self-gravitating disc. Duffy et al. provided results for the different co-moving box sizes: $25 h^{-1} \text{ Mpc}$ (high resolution), $50 h^{-1} \text{ Mpc}$ (middle resolution), and $100 h^{-1} \text{ Mpc}$ (low resolution). The simulations with the smallest box size were run to $z = 2$ and those with the larger box sizes were run to $z = 0$. Although Duffy et al. (2012) examined both cases of with and without AGN feedback, we adopted the former case since Duffy et al. already reported that the latter results in a large discrepancy between the simulation and observation.

- Genel et al. (2014, SIM) Genel et al. did not implement any H_2 formation models but assumed that one-third of the neutral gas of the galaxy is in the molecular phase to derive the lower limit for f_{H_2} of $z \sim 0$ galaxies formed in the Illustris simulation (Vogelsberger et al. 2013). Their estimated H_2 mass does not include the contribution of helium. They also assumed that all the neutral gas in a galactic disc is in the molecular phase to derive f_{H_2} of high- z galaxies and the upper limit of $z \sim 0$ galaxies. The Illustris uses a moving mesh code, AREPO (Springel 2010) and includes radiative cooling, heating from time-dependent UV background radiation, star formation (Springel & Hernquist 2003), mechanical feedback from SNe and thermal/mechanical/radiative feedbacks from AGNs (Springel et al. 2005a; Sijacki et al. 2007; Vogelsberger et al. 2013).

- Lagos et al. (2015, SIM) Lagos et al. implemented H_2 formation models as a post-process in EAGLE (Evolution and Assembly of GaLaxies and their Environments; Schaye et al. 2015), which is a cosmological numerical simulation that uses an N -body/SPH code, GADGET-3 (Springel et al. 2008). Here, H_2 formation is modelled according to two prescriptions depending on the local dust-to-gas ratio and the interstellar radiation field (Gnedin & Kravtsov 2011; Krumholz 2013). Their estimated H_2 mass does not include the contribution of helium. They considered radiative cooling (Wiersma et al. 2009; Schaye et al. 2015), photo-heating by cosmic microwave background, UV and X-ray background radiation (Haardt & Madau 2001), star formation (Schaye & Dalla Vecchia 2008), and thermal feedbacks from SNe (Dalla Vecchia & Schaye 2012) and AGN (Booth & Schaye 2009). We employed their $M_\star - f_{\text{mol}}$ relation (‘Ref-L100N1504’ model, see Fig. 5 of Lagos et al. 2015) calculated using the H_2 formation model of Gnedin & Kravtsov (2011).
- Obreschkow et al. (2009, SAM): They implemented

the pressure-based H_2 formation (partitioning) model (Blitz & Rosolowsky 2006; Leroy et al. 2008) as a post-process in the semi-analytical model, L-GALAXIES (Croton et al. 2006; De Lucia & Blaizot 2007), in which the dark matter halo and sub-halo merger trees are constructed from the Millennium Simulation (Springel et al. 2005b). With the L-GALAXIES, they implemented radiative cooling with the cooling function of Sutherland & Dopita (1993), photoionisation heating (Gnedin 2000; Kravtsov et al. 2004), star formation (Kauffmann 1996; Kennicutt 1989), and the feedbacks from SNe and AGN (Croton et al. 2006). We obtain their M_{H_2}/M_\star values from Fig. 9 of Popping et al. (2015) and recalculate f_{H_2} . Here, we mention that Popping et al. (2015) did not include the contribution from helium.

- Lagos et al. (2011b,a, SAM): Lagos et al. implemented both pressure-based (Blitz & Rosolowsky 2006) and metallicity-based (Krumholz et al. 2009a) H_2 formation models in the semi-analytical model, GALFORM (Cole et al. 2000; Benson et al. 2003; Baugh et al. 2005; Bower et al. 2006), in which the merger trees of dark matter halo were constructed using the Monte Carlo method (Lacey & Cole 1993). They considered the shock heating and radiative cooling (Sutherland & Dopita 1993) inside the dark matter halos, star formation (Lagos et al. 2011b; Kennicutt 1998b; Leroy et al. 2008; Bigiel et al. 2008; Krumholz et al. 2009a), and the feedbacks from SNe and AGN (Baugh et al. 2005; Bower et al. 2006). We obtain their M_{H_2}/M_\star values (pressure-based H_2 model and star formation model based on Bigiel et al. 2008) from Fig. 9 of Popping et al. (2015) and recalculate f_{H_2} . Here, we mention that Popping et al. (2015) did not include the contribution from helium.

- Fu et al. (2010, 2012, SAM): Fu et al. implemented both pressure-based (Blitz & Rosolowsky 2006) and metallicity-based (Krumholz et al. 2009a) H_2 formation models in the L-GALAXIES (Croton et al. 2006; De Lucia & Blaizot 2007) as is the case with Obreschkow et al. (2009). Unlike in Obreschkow et al. (2009), H_2 formation in this study is calculated in a self-consistent manner. The mass contribution from helium was taken into account (a factor of 1.4, Arnett 1996; Fu et al. 2010). Four kinds of star formation models were implemented: 1) ‘Bigiel’ (Bigiel et al. 2008; Leroy et al. 2008), 2) ‘Kennicutt’ (Kennicutt 1989, 1998b), 3) ‘Genzel’ (Genzel et al. 2010) and 4) ‘Krumholz’ (Krumholz et al. 2009b) models. They concluded that the ‘Bigiel’ model results in better agreement with the observed mass-metallicity relation among the four models. We employ their $M_\star - f_{\text{mol}}$ relation calculated using metallicity-based H_2 formation and the ‘Bigiel’ star formation model for a comparison purpose in this study.

- Popping et al. (2014, SAM): Popping et al. implemented pressure-based (Blitz & Rosolowsky 2006) and the metallicity-based (Gnedin et al. 2009) H_2 formation models in the Santa Cruz semi-analytical model (Somerville & Primack 1999; Somerville et al. 2008a, 2012), in which the dark matter halo merger tree was constructed using the Extended Press-Schechter formalism (Somerville & Kolatt 1999; Somerville et al. 2008b). They considered photoionization heating (Gnedin 2000; Kravtsov et al. 2004), radiative cooling (Sutherland & Dopita 1993; Somerville & Primack 1999),

star formation from molecular gas (Bigiel et al. 2008), and feedbacks from SNe and AGN. We obtain their M_{H_2}/M_* values (metallicity-based H_2 model and star formation model based on Bigiel et al. 2008) from Fig. 9 of Popping et al. (2015) and recalculate f_{H_2} . Here, we mention that Popping et al. (2015) did not include the contribution from helium.

We use the H_2 gas mass fraction $f_{\text{H}_2} = \frac{M_{\text{H}_2}}{M_{\text{H}_2} + M_*}$, which does not include the contribution from helium, instead of f_{mol} for a comparison between the observations and the theoretical predictions, since most theoretical studies considered here derived f_{H_2} . For the studies presenting f_{mol} instead of f_{H_2} , we recalculate M_{H_2} from M_{mol} using a conversion factor of 1.36 for Duffy et al. (2012) and Popping et al. (2012, indirect method), and 1.4 for Fu et al. (2012). Hereafter, the f_{H_2} calculated based on equation (3) and (4) is described as $f_{\text{H}_2, \text{P12, SF}}$ and the one calculated based on equation (5) and (6) is described as $f_{\text{H}_2, \text{P12}}$.

3.2 Discrepancy between observations and theoretical studies

Figure 2 compares the observed and predicted $M_* - f_{\text{H}_2}$ relations from theoretical studies. Here, we adopt $f_{\text{H}_2, \text{P12}}$ (black dot-dash lines in Fig. 2) as an observational reference for comparison with theoretical studies since the theoretical studies are not limited to star-forming galaxies. It should be noted that the theoretical studies did not apply any magnitude limits, which were applied to the observations. This uncertainty is discussed below. The predicted $M_* - f_{\text{H}_2}$ relations from SIMs (Duffy et al. 2012; Genel et al. 2014; Lagos et al. 2015) and SAMs (Obreschkow et al. 2009; Lagos et al. 2011b,a; Fu et al. 2010, 2012; Popping et al. 2014) are overlaid on the observed relation shown in Fig. 1.

The theoretical studies qualitatively reproduce the trends of the stellar-mass-dependent evolution of f_{H_2} where the less massive galaxies have higher f_{H_2} values than their massive counterparts; however, there is a ‘non-negligible’ gap between f_{H_2} from observations and theoretical studies (Popping et al. 2015). The f_{H_2} predictions from the theoretical studies appear to be consistent with the $f_{\text{H}_2, \text{P12}}$ values in the stellar mass range of $\sim 10^{10} - 10^{11} M_\odot$ in Fig. 2a, which is consistent with the results of a recent study (Lagos et al. 2015). However, the predicted f_{H_2} values by the SAMs of less massive ($< 10^{10} M_\odot$) are underestimated with respect to the observed values except for Obreschkow et al. (2009). The discrepancy between the observations and theoretical predictions is still observed even if we only consider nearby galaxies (Figs. 2a, b) in the stellar mass range of $10^{9.2} M_\odot < M_* < 10^{11} M_\odot$, wherein the observational completeness is 100 % (see section 2.2).

Obreschkow et al. (2009) predicted higher f_{H_2} values than the observation values for less massive galaxies, even though they used the same code (L-GALAXIES) as Fu et al. (2012). However, Obreschkow et al. (2009) implemented H_2 formation as a post-process whereas Fu et al. (2012) calculated H_2 formation in a self-consistent manner. This difference may explain the discrepancy between the two models, but Obreschkow et al. (2009) claimed that their galaxies with a stellar mass of $< 4 \times 10^9 M_\odot$ were typically

found in a halo with less than 100 particles, whose merging history could be followed over only a few time steps (De Lucia & Blaizot 2007).

There is a difference in the mass dependence of f_{H_2} , even though the SIMs and SAMs predict similar redshift evolution of the SMF of galaxies (see Fig. 4 of Somerville & Davé 2014). At all the redshift ranges ($0 < z < 2$), the SIMs predict more flat $M_* - f_{\text{H}_2}$ relations than those of the observations (upper panels of Fig. 2), whereas the SAMs predict kinks at the characteristic masses of $10^{10} - 10^{11} M_\odot$ (lower panels of Fig. 2). The difference in the prescriptions of H_2 formation is not likely the reason for this difference between the SAMs and SIMs since there is no clear difference among the SAMs depending on whether or not H_2 formation is implemented as a post-process (lower panels of Fig. 2) or depending on the models (pressure- or metallicity-based; Fu et al. 2012). Thus, the difference in modelling star formation and feedback may cause this difference. We discuss this gap between the SIMs and SAMs in section 4.2.

In the following paragraphs, we discuss possible causes for the f_{H_2} discrepancy between the observations and theoretical studies from an observational point of view. The observational studies essentially tend to be biased towards bright objects such as gas-rich objects and/or optically bright objects if the targets are selected based on large optical surveys. It has been claimed that the models reproduce the observational results relatively well if they take into account the sample selection criteria and observational sensitivities (Kauffmann et al. 2012; Popping et al. 2014). These studies showed that the predicted f_{H_2} value approaches the observed value if these observational conditions are considered, but there still seem to be discrepancies between observations and model predictions (see Fig. 11 in Popping et al. 2014). In addition, a gap between a semi-empirical model, as a proxy for observations, and theoretical predictions was also reported (Popping et al. 2015). This semi-empirical model couples a halo abundance matching model with a pressure-based H_2 formation model and is not affected by the observational limitations. However, we must pay attention to this observational limitation when comparing the observations and theoretical studies, especially for the less massive and higher- z galaxy samples, which are expected to be more biased to bright (gas-rich) objects compared to massive and low- z galaxy samples.

In addition to the observational bias, the uncertainty in the CO-to- H_2 conversion factor, α_{CO} , also contributes an additional error in the f_{H_2} estimate. Narayanan et al. (2012b) formulated α_{CO} as a function of the gas-phase metallicity and luminosity-weighted CO intensity. Narayanan et al. (2012a) showed that the observed f_{mol} value with Narayanan’s α_{CO} exhibits better agreement with the predicted values obtained with cosmological simulations. Even though the dispersion is reduced, certain systematic stellar-mass-dependent residuals still remain (see Fig. 3 in Narayanan et al. 2012a). Therefore, the observational causes alone may not be able to explain the discrepancy.

4 IMPLICATIONS FOR FEEDBACK MODELS

As described in section 3.2, there is a gap between the observed $M_\star - f_{\text{H}_2}$ relations and theoretically predicted relations. Although some fraction of this gap can be attributed to observational uncertainties such as the selection bias and variable α_{CO} , the gap still remains. This suggests that the gap might originate in the uncertainties of the theoretical models. In this section, we focus on the uncertainties of the feedback processes in the theoretical models⁶. The free parameters for the feedback processes are fixed to reproduce the observed SMF even though the SMF is not a direct outcome of the feedbacks alone, but a consequence of the several processes involved in galaxy evolution. This is because there is no definitive observational constraint for each feedback process. There might also be room for improvement in the H_2 and star formation models in terms of the molecule fraction and the K-S law, but they are set to meet the direct observational constraints for these processes.

To investigate the stellar mass and redshift dependence of each feedback process considered in theoretical studies, we construct an equilibrium model (EM) based on the study by Davé et al. (2012). In the following subsections, we briefly describe the EM (section 4.1), and subsequently, we examine the implications of the feedback processes through comparisons between the EMs and observations (section 4.2).

4.1 Equilibrium model for galaxy formation

The EM model is based on the idea that the simulated galaxies evolve in a quasi-equilibrium state (Bouché et al. 2010; Davé et al. 2012):

$$\dot{M}_{\text{in}} = \dot{M}_\star + \dot{M}_{\text{out}}, \quad (7)$$

where \dot{M}_{in} , \dot{M}_{out} , and \dot{M}_\star denote the mass inflow rate, mass outflow rate, and SFR, respectively. This model assumes that the stochastic variations in \dot{M}_{in} , arising due to factors such as mergers, are prone to return galaxies to equilibrium (see Davé et al. 2012, for details).

4.1.1 Stellar mass and gas fraction

In this section, we briefly introduce the formulation of stellar mass and gas fraction in the EM according to Davé et al. (2012). Integrating the equation $\dot{M}_\star = \dot{M}_{\text{in}} - \dot{M}_{\text{out}}$, we obtain the stellar mass $M_\star(M_{\text{h}}, z)$ as a function of the redshift z and halo mass M_{h} . The outflow rate is given as

$$\dot{M}_{\text{out}} = \eta \dot{M}_\star, \quad (8)$$

where the mass loading factor η is described as $\eta = (M_{\text{h}}/10^{12} \text{ M}_\odot)^{-1/3}$ (Davé et al. 2011a,b). The inflow rate into a galaxy \dot{M}_{in} is expressed as

⁶ Recent studies on galaxy formation based on the semi-analytic approach have suggested that the f_{H_2} gap between the observations and theoretical predictions decreases if the timescales for re-accretion of the ejected gas have a mass- and time-dependence (Henriques et al. 2013, 2015; Mitchell et al. 2014; White et al. 2015). Even though the physical origin for this treatment is not clear, some feedback processes may be attributed to changing the re-accretion timescale.

$$\dot{M}_{\text{in}} = \dot{M}_{\text{grav}} - \dot{M}_{\text{prev}} + \dot{M}_{\text{recyc}}, \quad (9)$$

where \dot{M}_{grav} , \dot{M}_{prev} , and \dot{M}_{recyc} denote the baryonic inflow rate into a galaxy's halo, rate at which material ends up in the gaseous halo of the galaxy, and return infall rate, respectively. These are expressed as

$$\dot{M}_{\text{grav}} = f_{\text{b}} \dot{M}_{\text{h}}, \quad (10)$$

$$\dot{M}_{\text{prev}} = (1 - \zeta) \dot{M}_{\text{grav}}, \quad (11)$$

$$\dot{M}_{\text{recyc}} = \frac{\alpha_{\text{Z}}}{1 - \alpha_{\text{Z}}} \zeta \dot{M}_{\text{grav}}. \quad (12)$$

Here, \dot{M}_{h} denotes the halo mass growth rate as given by

$$\dot{M}_{\text{h}} = 25.3 \left(\frac{M_{\text{h}}}{10^{12} \text{ M}_\odot} \right)^{1.1} (1 + 1.65z) \sqrt{\Omega_{\text{m}}(1+z)^3 + \Omega_{\Lambda}}, \quad (13)$$

which is derived from cosmological N -body simulations (Fakhouri et al. 2010), f_{b} represents the cosmic baryon fraction (0.17), Ω_{m} the matter density parameter (0.3), Ω_{Λ} the dark energy density parameter (0.7), ζ the preventive feedback parameter (a product of four feedback parameters, $\zeta_{\text{PHOTO}} \zeta_{\text{GRAV}} \zeta_{\text{QUENCH}} \zeta_{\text{WIND}}$; see the next subsection for explanations on each feedback), and α_{Z} the metallicity ratio of inflow gas and ISM⁷ $\alpha_{\text{Z}} = (0.3 - 0.1z)(M_\star/10^{10} \text{ M}_\odot)^{0.25}$ (Davé et al. 2012). Substituting these equations into equation (9) yields

$$\dot{M}_{\text{in}} = \frac{\zeta}{1 - \alpha_{\text{Z}}} \dot{M}_{\text{grav}}. \quad (14)$$

If we substitute equations (8) and (14) into equation (7), the SFR can be written as

$$\dot{M}_\star = \frac{\zeta \dot{M}_{\text{grav}}}{(1 + \eta)(1 - \alpha_{\text{Z}})}. \quad (15)$$

In the EM, if M_\star and \dot{M}_\star are known via the procedure described above, the gas fraction of a galaxy is given by

$$f_{\text{gas}} \equiv \frac{M_{\text{gas}}}{M_{\text{gas}} + M_\star} = \frac{1}{1 + (t_{\text{dep}} \dot{M}_\star / M_\star)^{-1}}, \quad (16)$$

where $t_{\text{dep}} \equiv M_{\text{gas}} / \dot{M}_\star$ denotes the depletion time of the gas component by star formation. We use the Hubble time t_{H} to parameterise $t_{\text{dep}} = 0.4 t_{\text{H}} (M_\star/10^{10} \text{ M}_\odot)^{-0.3}$ as discussed in Davé et al. (2012).

4.1.2 Preventive feedback parameters

Each preventive feedback parameter⁸ ζ depends on the halo mass M_{h} and redshift z . The EM considers four feedback processes as follows:

- ζ_{PHOTO} , photoionising heating (hereafter PHOTO): An ultraviolet background radiation heats the halo gas of galaxies. It effectively works in less massive systems since less

⁷ Davé et al. (2012) used $\alpha_{\text{Z}} = (0.5 - 0.1z)(M_\star/10^{10} \text{ M}_\odot)^{0.25}$ but we use $\alpha_{\text{Z}} = (0.3 - 0.1z)(M_\star/10^{10} \text{ M}_\odot)^{0.25}$ to prevent the results from being diverged. This difference is because some of the equations, which are not fully based on physics or ab initio simulations, were not presented in Davé et al. (2012) (such as $M_{\text{q}}(z)$ for equation (19) and $M_{\text{wind}}(z)$ for equation (20)); hence, we must formulate them by ourselves.

⁸ In Davé's model, all feedbacks are modeled in 'preventive' manner but some are represented as 'ejective' feedback.

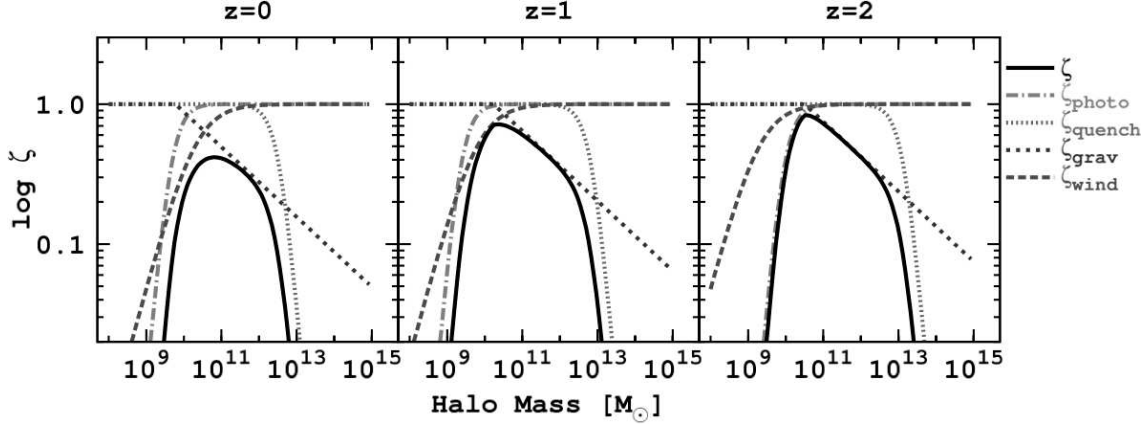


Figure 3. Preventive feedback parameters as a function of halo mass at $z = 0, 1.0$, and 2.0 . The total preventive feedback parameter ζ (black solid line) is the product of four preventive feedback parameters, ζ_{PHOTO} (gray dashed lines), ζ_{GRAV} (gray dotted lines), ζ_{QUENCH} (gray short-dotted lines), and ζ_{WIND} (gray dashed lines).

massive galaxies cannot confine or acquire heated (photoionised) gas due to their shallow potential wells (e.g. Gnedin 2000; Okamoto et al. 2008).

$$\zeta_{\text{PHOTO}} = \left[1 + \frac{1}{3} \left(\frac{M_\gamma(z)}{M_{\text{halo}}} \right)^2 \right]^{-1.5}, \quad (17)$$

where the photosuppression mass, $M_\gamma(z)$ is taken from Fig. B1 of Okamoto et al. (2008).

- ζ_{GRAV} , virial shock heating during gas accretion (hereafter GRAV): It effectively works in massive systems since the sparsity and high virial temperature of the halo gas in massive systems prevent the halo gas from accreting onto the galaxy (e.g. Faucher-Giguère et al. 2011).

$$\zeta_{\text{GRAV}} = \text{MIN} \left[1, 0.47 \left(\frac{1+z}{4} \right)^{0.38} \left(\frac{M_{\text{halo}}}{10^{12} \text{ M}_\odot} \right)^{-0.25} \right]. \quad (18)$$

- ζ_{QUENCH} , heating up the ISM and/or halo gas and preventing cooling flow from the halo due to supermassive black hole (BH) growth (or AGN feedback; hereafter QUENCH): This feedback works in massive systems (Croton et al. 2006; Gabor et al. 2011).

$$\zeta_{\text{QUENCH}} = \left[1 + \frac{1}{3} \left(\frac{M_{\text{halo}}}{M_q(z)} \right)^2 \right]^{-1.5}, \quad (19)$$

where the quenching mass is given by $M_q(z) = 10^{12+0.3(1+z)} \text{ M}_\odot$. We formulate $M_q(z)$ so as to represent the red line in Fig. 1 of Davé et al. (2012).

- ζ_{WIND} , heating of surrounding gas by SNe (hereafter WIND): it effectively works in less massive systems since ubiquitous SNe wind tends to blow out the gas in less massive galaxies due to their shallow potential wells (e.g. Oppenheimer et al. 2010).

$$\zeta_{\text{WIND}} = \left[1 + \frac{1}{50} \left(\frac{M_{\text{wind}}(z)}{M_{\text{halo}}} \right) \right]^{-1}, \quad (20)$$

where the wind mass is given by $M_{\text{wind}} = 10^{12.5-0.5(1+z)} \text{ M}_\odot$. We formulate M_{wind} so as to represent the blue line in Fig. 1 of Davé et al. (2012).

We present the preventive feedback parameters as a function of halo mass in Fig. 3 (see also Fig.1 of Davé et al. 2012).

4.2 Comparisons between the EMs and observations

We compare the observed $M_\star - f_{\text{gas}}$ relations with the predictions from the EMs in Fig. 4. Here, we use Popping's $M_\star - f_{\text{gas}}$ relation as the observational reference (Popping et al. in prep.), which is described below:

$$f_{\text{gas,P12}} = \frac{1}{\exp(\log M_\star - E)/F + 1}, \quad (21)$$

where

$$E = 9.04 \left(1 + \frac{z}{1.76} \right)^{0.24}, \quad F = 0.53(1+z)^{-0.91}. \quad (22)$$

We use the $M_\star - f_{\text{gas}}$ relation because Dave's EMs do not consider H_2 formation. To clarify the contribution from each feedback process, five conditions are considered: 1) all feedback processes are considered, 2) PHOTO is not considered, 3) GRAV is not considered, 4) QUENCH is not considered, and 5) WIND is not considered.

From Fig. 4, we can confirm the stellar-mass dependence and observe the degree of influence of each feedback process as expected from Fig. 3. For less massive galaxies (but $> 10^{9.2} \text{ M}_\odot$ according to observational completeness), the theoretically predicted f_{gas} value approaches the observation value at $z = 0$ (Fig. 4a), but it is considerably lower than the observation value even if we exclude the PHOTO and WIND feedback processes. On the other hand, the QUENCH and GRAV feedback processes work well for massive galaxies. The stellar-mass dependence of f_{gas} in the high-mass range (but $< 10^{11} \text{ M}_\odot$ according to observational completeness) appears to be different in that there is a knee around $M_\star \sim 10^{10.5} \text{ M}_\odot$ in the EM as opposed to a monotonic decrease in observations; however, it is not conclusive because these are consistent within the typical dispersion of the observed relation.

From Fig. 2, we observe that theoretical studies tend to predict lower gas fractions than observations, particularly in less massive and massive galaxies. Our result suggests that

the feedback models implemented in the theoretical studies are clearly required. However, the physical ingredients in these models are still insufficient to correctly reproduce the available observations. One requirement is to consider a feedback model that quenches star formation but retains the cold-gas component in galaxies.

The EM predicts a stellar-mass dependence of f_{gas} similar to that of f_{H_2} predicted by the SAMs, rather than the SIMs; there is a kink at the characteristic stellar mass. The $M_\star - f_{\text{gas}}$ relations predicted by the EMs without ζ_{GRAV} or ζ_{QHENCH} become flat, similar to the predictions of the SIMs. The observations indicate that the $M_\star - f_{\text{gas}}$ or $M_\star - f_{\text{H}_2}$ relations are similar to the predictions of the EM and SAMs at higher redshifts, while these relations are similar to the SIMs at lower redshifts. The virial shock heating is expected to be included in the SIMs naturally, but AGN feedback is implemented as an ad-hoc model. If the observed f_{gas} evolution in the high-mass range of Popping et al. (2012) is correct, our comparison suggests a more drastic redshift evolution of AGN feedback than the SIMs, i.e. a stronger AGN feedback for a high redshift and a weaker one for a low redshift. However, the details regarding the modelling of AGN feedback are beyond the scope of this paper.

Some recent studies have emphasised the relevance of the feedback processes, which suppress star formation while simultaneously preserving the cold gas (Makiya et al. 2014; Morokuma-Matsui et al. 2015). Our results showed that the EMs and the SAMs tend to underestimate f_{gas} or f_{H_2} in less massive and massive galaxies. There is a larger gap between the observations and theoretical predictions for less massive galaxies in Fig. 4a ($M_\star - f_{\text{gas}}$ relation) than in Fig. 2a ($M_\star - f_{\text{H}_2}$ relation). This larger gap in f_{gas} in less massive galaxies suggests a lot of ejection of cold gas by SN feedback modeled in the theoretical studies. The gap may be reduced if we consider the suppression of H_2 formation instead of the ejection of total cold gas.

Makiya et al. (2014) implemented a star formation law with a feedback depending on galaxy-scale mean dust opacity and metallicity in SAM and succeeded in reproducing the faint-end slopes of galaxy luminosity functions at $z = 0$ with a *reasonable* strength of the SN feedback. In their model, star formation in less massive galaxies is suppressed because such galaxies tend to have lower metallicity, lower surface density, and thus, lower H_2 fraction. For massive galaxies, morphological quenching is one of the important processes, which can quench star formation even in the presence of a gas component. Martig et al. (2009) showed that star formation is suppressed once the central spheroidal component becomes sufficiently massive to stabilise the galactic disc against local gravitational instability. Some observational studies suggested that morphological quenching is in action in the early-type galaxies (Martig et al. 2013; Morokuma-Matsui et al. 2015).

5 SUMMARY

Galaxy formation models are constructed so as to reproduce the observed SMF of galaxies by blowing out and/or heating up the cold-gas component to quench further star formation, particularly in less massive and massive systems. To investigate whether the current galaxy formation mod-

els also reproduce the observed properties of the cold-gas component of galaxies, we compare the observed and theoretically predicted evolution of the molecular gas fraction with respect to the total baryonic mass as a function of stellar mass (i.e. the $M_\star - f_{\text{mol}}$ or $M_\star - f_{\text{H}_2}$ relations). Our main findings are as follows:

- (i) The evolution of the observed $M_\star - f_{\text{mol}}$ relation shows a stellar-mass dependent evolution; massive galaxies have largely depleted their molecular gas at $z = 1$, whereas less massive galaxies tend to convert molecular gas into stars in the regime of $0 < z < 1$.
- (ii) The current cosmological hydrodynamic simulations and semi-analytical models for galaxy formation succeed in ‘qualitatively’ reproducing the $M_\star - f_{\text{H}_2}$ relation evolution in the regime of $0 < z < 2$ where less massive galaxies are always more gas-rich than massive galaxies.
- (iii) There is a non-negligible gap between the observed and theoretically predicted $M_\star - f_{\text{H}_2}$ relations. The predicted f_{mol} value is more than two times smaller than the observed value at most, particularly in less massive ($< 10^{10} M_\odot$) and massive galaxies ($> 10^{11} M_\odot$). Accordingly, for this gap, the use of feedback models could be required, which quench star formation but retain the cold-gas component.
- (iv) The observed redshift evolution of the cold gas mass fraction in massive galaxies suggests a more drastic evolution of AGN feedback than the one implemented in the hydrodynamic simulations, i.e. a stronger AGN feedback in higher redshift ($z > 1$) and a weaker one in lower redshift ($z < 1$).
- (v) The SMF of galaxies alone is not sufficient for constraining the galaxy formation models and the $M_\star - f_{\text{mol}}$ relation forms one of the important observational constraints on feedback processes implemented in galaxy-formation models.

It is to be noted that we adopted the indirect estimates of f_{mol} using the optical survey data (Popping et al. 2012) for comparison with the galaxy formation models in this study. To form a definitive conclusion regarding the f_{mol} evolution of galaxies (particularly less massive and massive galaxies), it is necessary to directly measure the cold gas mass of galaxies over wide ranges of stellar mass and redshift. The mass function of the stellar component is of course a basic observed constraint, which must be satisfied for the models. The cold-gas component is also an important component in the baryonic cycle of galaxies. A combination of the observational constraints on stellar and cold gas components will aid in sketching a complete scenario of galaxy formation and evolution. Observations with forthcoming facilities such as the ALMA, the NOEMA, and the SKA, will allow us to explore the statistical properties and evolution of cold-gas components in galaxies, such as H_1 and H_2 mass functions, as well as the $M_\star - f_{\text{mol}}$ relation.

ACKNOWLEDGMENTS

We thank the referee, Gergő Popping, for a very thorough report which led to a substantial improvement of the paper. JB was supported by JSPS Grant-in-Aid for Young Scientists (B) Grand Number 26800099. We would like to thank Takeshi Okamoto, Masahiro Nagashima and Ryu Makiya for

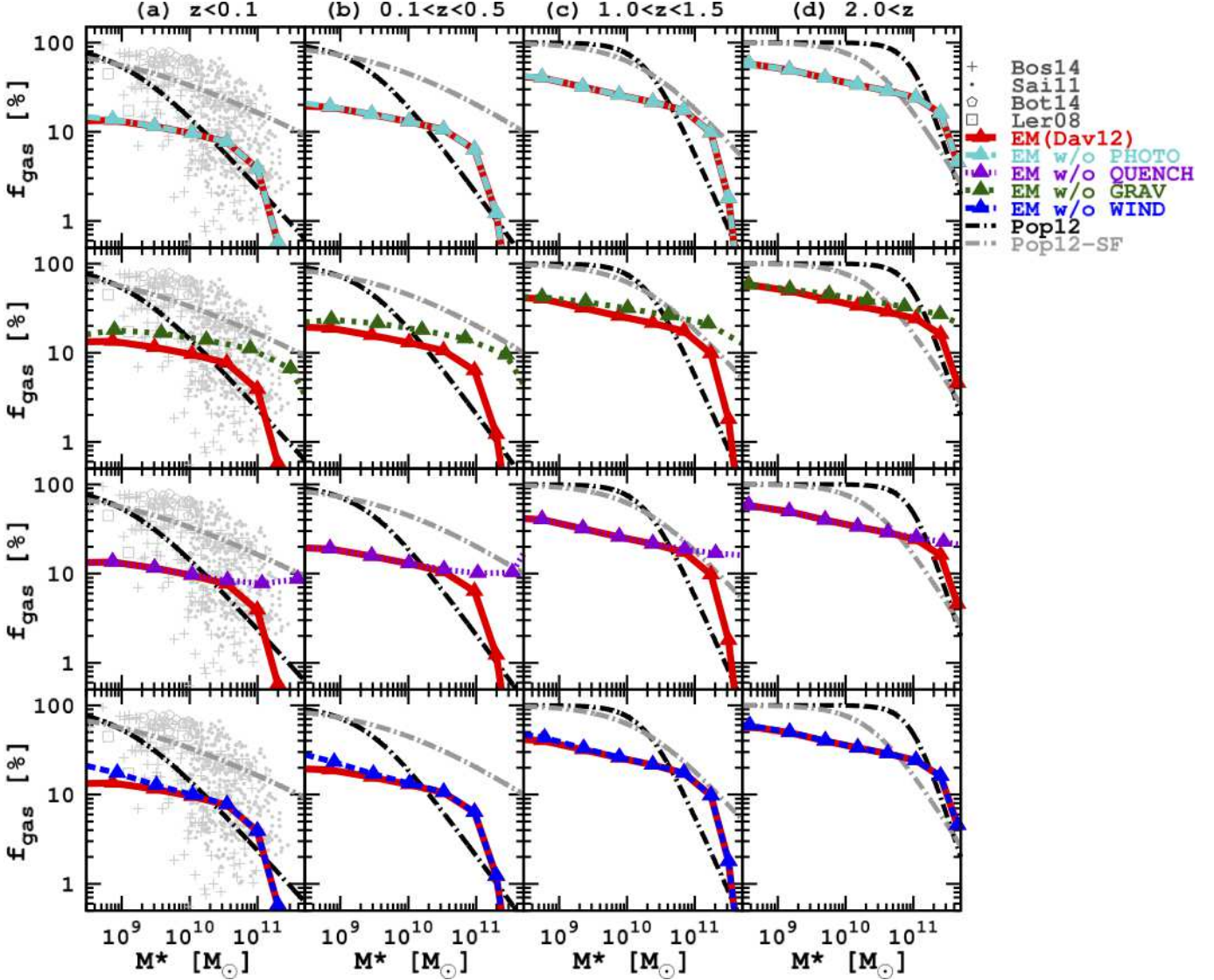


Figure 4. Total gas fraction f_{gas} as a function of stellar mass and redshift (a: $z < 0.1$, b: $0.1 < z < 0.5$, c: $1.0 < z < 1.5$ and d: $2.0 < z$). The black and grey dot-dash lines indicate the $M_{\star} - f_{\text{gas}}$ relation based on the K-S law for whole and star-forming samples in Popping et al. (2012). The redshifts of the equations for $f_{\text{mol,P12,SF}}$ and $f_{\text{mol,P12}}$ are 0.025 for (a), 0.3 for (b), 1.25 for (c), and 2.2 for (d). The lines with filled triangles indicate the results of the ‘equilibrium model (EM)’ by Davé et al. (2012) (red solid lines: model with all feedbacks, light-blue dot-dashed lines: model without photoionising feedback (PHOTO), green dotted lines: model without shock-heating during accretion (GRAV), purple short-dotted lines: model without quenching associated with black hole growth (QUENCH), and blue dashed lines: model without additional feedback associated with wind (WIND)). On each plot, we show the result of EM calculations at $z = 0$ in (a), $z = 0.2$ in (b), $z = 1$ in (c) and $z = 2$ in (d). The $M_{\star} - f_{\text{gas}}$ relations from the direct observations (HI and CO) are plotted as a reference (Leroy et al. 2008; Saintonge et al. 2011a; Boselli et al. 2014; Bothwell et al. 2014).

productive discussions, and Ross Burns, Daisuke Iono and Editage (www.editage.jp) for English language editing.

Funding for SDSS-III has been provided by the Alfred P. Sloan Foundation, the Participating Institutions, the National Science Foundation, and the U.S. Department of Energy Office of Science. The SDSS-III web site is (<http://www.sdss3.org/>). SDSS-III is managed by the Astrophysical Research Consortium for the Participating Institutions of the SDSS-III Collaboration including the University of Arizona, the Brazilian Participation Group, Brookhaven National Laboratory, Carnegie Mellon University, University of Florida, the French Participation Group, the German Participation Group, Harvard Univer-

sity, the Instituto de Astrofísica de Canarias, the Michigan State/Notre Dame/JINA Participation Group, Johns Hopkins University, Lawrence Berkeley National Laboratory, Max Planck Institute for Astrophysics, Max Planck Institute for Extraterrestrial Physics, New Mexico State University, New York University, Ohio State University, Pennsylvania State University, University of Portsmouth, Princeton University, the Spanish Participation Group, University of Tokyo, University of Utah, Vanderbilt University, University of Virginia, University of Washington, and Yale University.

REFERENCES

- Abazajian K. N. et al., 2009, *ApJS*, 182, 543
- Ahn C. P. et al., 2014, *ApJS*, 211, 17
- Arnett D., 1996, *Supernovae and Nucleosynthesis: An Investigation of the History of Matter from the Big Bang to the Present*
- Bauermeister A., Blitz L., Bolatto A., Bureau M., Teuben P., Wong T., Wright M., 2013, *ApJ*, 763, 64
- Baugh C. M., Lacey C. G., Frenk C. S., Granato G. L., Silva L., Bressan A., Benson A. J., Cole S., 2005, *MNRAS*, 356, 1191
- Benson A. J., Bower R. G., Frenk C. S., Lacey C. G., Baugh C. M., Cole S., 2003, *ApJ*, 599, 38
- Berry M., Somerville R. S., Haas M. R., Gawiser E., Maller A., Popping G., Trager S. C., 2014, *MNRAS*, 441, 939
- Bigiel F., Leroy A., Walter F., Brinks E., de Blok W. J. G., Madore B., Thornley M. D., 2008, *AJ*, 136, 2846
- Bird S., Vogelsberger M., Haehnelt M., Sijacki D., Genel S., Torrey P., Springel V., Hernquist L., 2014, *MNRAS*, 445, 2313
- Blanton M. R., Roweis S., 2007, *AJ*, 133, 734
- Blitz L., Rosolowsky E., 2004, *ApJL*, 612, L29
- Blitz L., Rosolowsky E., 2006, *ApJ*, 650, 933
- Bolatto A. D., Wolfire M., Leroy A. K., 2013, *ARA&A*, 51, 207
- Booth C. M., Schaye J., 2009, *MNRAS*, 398, 53
- Boselli A., Cortese L., Boquien M., 2014, *A&A*, 564, A65
- Bothwell M. S. et al., 2014, *MNRAS*, 445, 2599
- Bouché N. et al., 2010, *ApJ*, 718, 1001
- Bower R. G., Benson A. J., Malbon R., Helly J. C., Frenk C. S., Baugh C. M., Cole S., Lacey C. G., 2006, *MNRAS*, 370, 645
- Brinchmann J., Charlot S., White S. D. M., Tremonti C., Kauffmann G., Heckman T., Brinkmann J., 2004, *MNRAS*, 351, 1151
- Bruzual G., Charlot S., 2003, *MNRAS*, 344, 1000
- Carilli C. L., Walter F., 2013, *ARA&A*, 51, 105
- Catinella B., Haynes M. P., Giovanelli R., Gardner J. P., Connolly A. J., 2008, *ApJL*, 685, L13
- Chabrier G., 2003, *PASP*, 115, 763
- Chomiuk L., Povich M. S., 2011, *AJ*, 142, 197
- Christensen C., Quinn T., Governato F., Stilp A., Shen S., Wadsley J., 2012, *MNRAS*, 425, 3058
- Ciesla L. et al., 2014, *A&A*, 565, A128
- Cole S., Lacey C. G., Baugh C. M., Frenk C. S., 2000, *MNRAS*, 319, 168
- Cole S. et al., 2001, *MNRAS*, 326, 255
- Conroy C., Wechsler R. H., 2009, *ApJ*, 696, 620
- Cortese L. et al., 2012, *A&A*, 544, A101
- Cortese L. et al., 2014, *MNRAS*, 440, 942
- Croton D. J. et al., 2006, *MNRAS*, 365, 11
- Daddi E. et al., 2010, *ApJ*, 713, 686
- Daddi E., Cimatti A., Renzini A., Fontana A., Mignoli M., Pozzetti L., Tozzi P., Zamorani G., 2004, *ApJ*, 617, 746
- Dalla Vecchia C., Schaye J., 2008, *MNRAS*, 387, 1431
- Dalla Vecchia C., Schaye J., 2012, *MNRAS*, 426, 140
- Dannerbauer H., Daddi E., Riechers D. A., Walter F., Carilli C. L., Dickinson M., Elbaz D., Morrison G. E., 2009, *ApJL*, 698, L178
- Davé R., Finlator K., Oppenheimer B. D., 2011a, *MNRAS*, 416, 1354
- Davé R., Finlator K., Oppenheimer B. D., 2012, *MNRAS*, 421, 98
- Davé R., Oppenheimer B. D., Finlator K., 2011b, *MNRAS*, 415, 11
- De Lucia G., Blaizot J., 2007, *MNRAS*, 375, 2
- Dekel A., Sari R., Ceverino D., 2009, *ApJ*, 703, 785
- Dekel A., Silk J., 1986, *ApJ*, 303, 39
- Duffy A. R., Kay S. T., Battye R. A., Booth C. M., Dalla Vecchia C., Schaye J., 2012, *MNRAS*, 420, 2799
- Efstathiou G., 1992, *MNRAS*, 256, 43P
- Fakhouri O., Ma C.-P., Boylan-Kolchin M., 2010, *MNRAS*, 406, 2267
- Faucher-Giguère C.-A., Kereš D., Ma C.-P., 2011, *MNRAS*, 417, 2982
- Fernández X. et al., 2013, *ApJL*, 770, L29
- Förster Schreiber N. M. et al., 2009, *ApJ*, 706, 1364
- Freudling W. et al., 2011, *ApJ*, 727, 40
- Fu J., Guo Q., Kauffmann G., Krumholz M. R., 2010, *MNRAS*, 409, 515
- Fu J., Kauffmann G., Li C., Guo Q., 2012, *MNRAS*, 424, 2701
- Fumagalli M., Krumholz M. R., Hunt L. K., 2010, *ApJ*, 722, 919
- Gabor J. M., Davé R., Oppenheimer B. D., Finlator K., 2011, *MNRAS*, 417, 2676
- Geach J. E., Smail I., Moran S. M., MacArthur L. A., Lagos C. d. P., Edge A. C., 2011, *ApJL*, 730, L19
- Geach J. E., Smail I., Moran S. M., Treu T., Ellis R. S., 2009, *ApJ*, 691, 783
- Genel S. et al., 2014, *MNRAS*, 445, 175
- Genzel R. et al., 2010, *MNRAS*, 407, 2091
- Gnedin N. Y., 2000, *ApJ*, 542, 535
- Gnedin N. Y., Kravtsov A. V., 2011, *ApJ*, 728, 88
- Gnedin N. Y., Tassis K., Kravtsov A. V., 2009, *ApJ*, 697, 55
- Haardt F., Madau P., 2001, in *Clusters of Galaxies and the High Redshift Universe Observed in X-rays*, Neumann D. M., Tran J. T. V., eds., p. 64
- Helfer T. T., Thornley M. D., Regan M. W., Wong T., Sheth K., Vogel S. N., Blitz L., Bock D. C.-J., 2003, *ApJS*, 145, 259
- Henriques B. M. B., White S. D. M., Thomas P. A., Angulo R., Guo Q., Lemson G., Springel V., Overzier R., 2015, *MNRAS*, 451, 2663
- Henriques B. M. B., White S. D. M., Thomas P. A., Angulo R. E., Guo Q., Lemson G., Springel V., 2013, *MNRAS*, 431, 3373
- Ikeuchi S., 1986, *Ap&SS*, 118, 509
- Ilbert O. et al., 2010, *ApJ*, 709, 644
- Kauffmann G., 1996, *MNRAS*, 281, 475
- Kauffmann G., Colberg J. M., Diaferio A., White S. D. M., 1999, *MNRAS*, 303, 188
- Kauffmann G. et al., 2003, *MNRAS*, 346, 1055
- Kauffmann G. et al., 2012, *MNRAS*, 422, 997
- Kennicutt R. C., Evans N. J., 2012, *ARA&A*, 50, 531
- Kennicutt, Jr. R. C., 1989, *ApJ*, 344, 685
- Kennicutt, Jr. R. C., 1998a, *ARA&A*, 36, 189
- Kennicutt, Jr. R. C., 1998b, *ApJ*, 498, 541
- Kereš D., Katz N., Weinberg D. H., Davé R., 2005, *MNRAS*, 363, 2
- Khochfar S., Ostriker J. P., 2008, *ApJ*, 680, 54
- Kochanek C. S. et al., 2001, *ApJ*, 560, 566

- Kravtsov A. V., Gnedin O. Y., Klypin A. A., 2004, *ApJ*, 609, 482
- Kroupa P., 2001, *MNRAS*, 322, 231
- Krumholz M. R., 2013, *MNRAS*, 436, 2747
- Krumholz M. R., McKee C. F., Tumlinson J., 2008, *ApJ*, 689, 865
- Krumholz M. R., McKee C. F., Tumlinson J., 2009a, *ApJ*, 693, 216
- Krumholz M. R., McKee C. F., Tumlinson J., 2009b, *ApJ*, 699, 850
- Lacey C., Cole S., 1993, *MNRAS*, 262, 627
- Lagos C. D. P., Baugh C. M., Lacey C. G., Benson A. J., Kim H.-S., Power C., 2011a, *MNRAS*, 418, 1649
- Lagos C. d. P. et al., 2015, *ArXiv e-prints*
- Lagos C. D. P., Lacey C. G., Baugh C. M., Bower R. G., Benson A. J., 2011b, *MNRAS*, 416, 1566
- Larson R. B., 1974, *MNRAS*, 169, 229
- Leitner S. N., 2012, *ApJ*, 745, 149
- Leroy A. K., Walter F., Brinks E., Bigiel F., de Blok W. J. G., Madore B., Thornley M. D., 2008, *AJ*, 136, 2782
- Lu Y., Mo H. J., Wechsler R. H., 2015, *MNRAS*, 446, 1907
- Madau P., Dickinson M., 2014, *ARA&A*, 52, 415
- Magdis G. E. et al., 2012a, *ApJ*, 760, 6
- Magdis G. E. et al., 2012b, *ApJL*, 758, L9
- Makiya R., Totani T., Kobayashi M. A. R., Nagashima M., Takeuchi T. T., 2014, *MNRAS*, 441, 63
- Mancini C. et al., 2011, *ApJ*, 743, 86
- Martig M., Bournaud F., Teyssier R., Dekel A., 2009, *ApJ*, 707, 250
- Martig M. et al., 2013, *MNRAS*, 432, 1914
- Mitchell P. D., Lacey C. G., Cole S., Baugh C. M., 2014, *MNRAS*, 444, 2637
- Mo H. J., Yang X., van den Bosch F. C., Katz N., 2005, *MNRAS*, 363, 1155
- Moran S. M., Ellis R. S., Treu T., Smith G. P., Rich R. M., Smail I., 2007, *ApJ*, 671, 1503
- Morokuma-Matsui K., Baba J., Sorai K., Kuno N., 2015, *PASJ*, 67, 36
- Nagashima M., Yahagi H., Enoki M., Yoshii Y., Gouda N., 2005, *ApJ*, 634, 26
- Narayanan D., Bothwell M., Davé R., 2012a, *MNRAS*, 426, 1178
- Narayanan D., Krumholz M. R., Ostriker E. C., Hernquist L., 2012b, *MNRAS*, 421, 3127
- Navarro J. F., Steinmetz M., 1997, *ApJ*, 478, 13
- Noeske K. G. et al., 2007, *ApJL*, 660, L43
- Obreschkow D., Croton D., De Lucia G., Khochfar S., Rawlings S., 2009, *ApJ*, 698, 1467
- Okamoto T., Gao L., Theuns T., 2008, *MNRAS*, 390, 920
- Okamoto T., Shimizu I., Yoshida N., 2014, *PASJ*, 66, 70
- Oppenheimer B. D., Davé R., Kereš D., Fardal M., Katz N., Kollmeier J. A., Weinberg D. H., 2010, *MNRAS*, 406, 2325
- Popping G., Behroozi P. S., Peebles M. S., 2015, *MNRAS*, 449, 477
- Popping G., Caputi K. I., Somerville R. S., Trager S. C., 2012, *MNRAS*, 425, 2386
- Popping G., Somerville R. S., Trager S. C., 2014, *MNRAS*, 442, 2398
- Rahmati A., Pawlik A. H., Raičević M., Schaye J., 2013a, *MNRAS*, 430, 2427
- Rahmati A., Schaye J., 2014, *MNRAS*, 438, 529
- Rahmati A., Schaye J., Bower R. G., Crain R. A., Furlong M., Schaller M., Theuns T., 2015, *ArXiv e-prints*
- Rahmati A., Schaye J., Pawlik A. H., Raičević M., 2013b, *MNRAS*, 431, 2261
- Rees M. J., Ostriker J. P., 1977, *MNRAS*, 179, 541
- Rhee J., Zwaan M. A., Briggs F. H., Chengalur J. N., Lah P., Oosterloo T., van der Hulst T., 2013, *MNRAS*, 435, 2693
- Saintonge A. et al., 2011a, *MNRAS*, 415, 32
- Saintonge A. et al., 2011b, *MNRAS*, 415, 61
- Saintonge A. et al., 2013, *ApJ*, 778, 2
- Santini P. et al., 2014, *A&A*, 562, A30
- Schaye J. et al., 2015, *MNRAS*, 446, 521
- Schaye J., Dalla Vecchia C., 2008, *MNRAS*, 383, 1210
- Schaye J. et al., 2010, *MNRAS*, 402, 1536
- Scoville N. et al., 2007, *ApJS*, 172, 1
- Scoville N. et al., 2014, *ApJ*, 783, 84
- Scoville N. et al., 2015, *ArXiv e-prints*
- Sijacki D., Springel V., Di Matteo T., Hernquist L., 2007, *MNRAS*, 380, 877
- Silk J., Mamon G. A., 2012, *Research in Astronomy and Astrophysics*, 12, 917
- Somerville R. S. et al., 2008a, *ApJ*, 672, 776
- Somerville R. S., Davé R., 2014, *ArXiv e-prints*
- Somerville R. S., Gilmore R. C., Primack J. R., Domínguez A., 2012, *MNRAS*, 423, 1992
- Somerville R. S., Hopkins P. F., Cox T. J., Robertson B. E., Hernquist L., 2008b, *MNRAS*, 391, 481
- Somerville R. S., Kolatt T. S., 1999, *MNRAS*, 305, 1
- Somerville R. S., Popping G., Trager S. C., 2015, *ArXiv e-prints*
- Somerville R. S., Primack J. R., 1999, *MNRAS*, 310, 1087
- Springel V., 2010, *MNRAS*, 401, 791
- Springel V., Di Matteo T., Hernquist L., 2005a, *MNRAS*, 361, 776
- Springel V., Hernquist L., 2003, *MNRAS*, 339, 289
- Springel V. et al., 2008, *MNRAS*, 391, 1685
- Springel V. et al., 2005b, *Nature*, 435, 629
- Sutherland R. S., Dopita M. A., 1993, *ApJS*, 88, 253
- Tacconi L. J. et al., 2010, *Nature*, 463, 781
- Tacconi L. J. et al., 2013, *ApJ*, 768, 74
- Thompson R., Nagamine K., Jaacks J., Choi J.-H., 2014, *ApJ*, 780, 145
- Tomassetti M., Porciani C., Romano-Díaz E., Ludlow A. D., 2015, *MNRAS*, 446, 3330
- Tremonti C. A. et al., 2004, *ApJ*, 613, 898
- Vogelsberger M., Genel S., Sijacki D., Torrey P., Springel V., Hernquist L., 2013, *MNRAS*, 436, 3031
- Vogelsberger M. et al., 2014, *MNRAS*, 444, 1518
- White C. E., Somerville R. S., Ferguson H. C., 2015, *ApJ*, 799, 201
- Wiersma R. P. C., Schaye J., Smith B. D., 2009, *MNRAS*, 393, 99
- Wuyts S. et al., 2011, *ApJ*, 738, 106
- Zibetti S., Charlot S., Rix H.-W., 2009, *MNRAS*, 400, 1181